Journal of Physics: Conference Series

Numerical investigation of volume of fluid and level set interface capturing methods for bubble growth and detachment

To cite this article: Abdulaleem Albadawi *et al* 2012 *J. Phys.: Conf. Ser.* **395** 012166

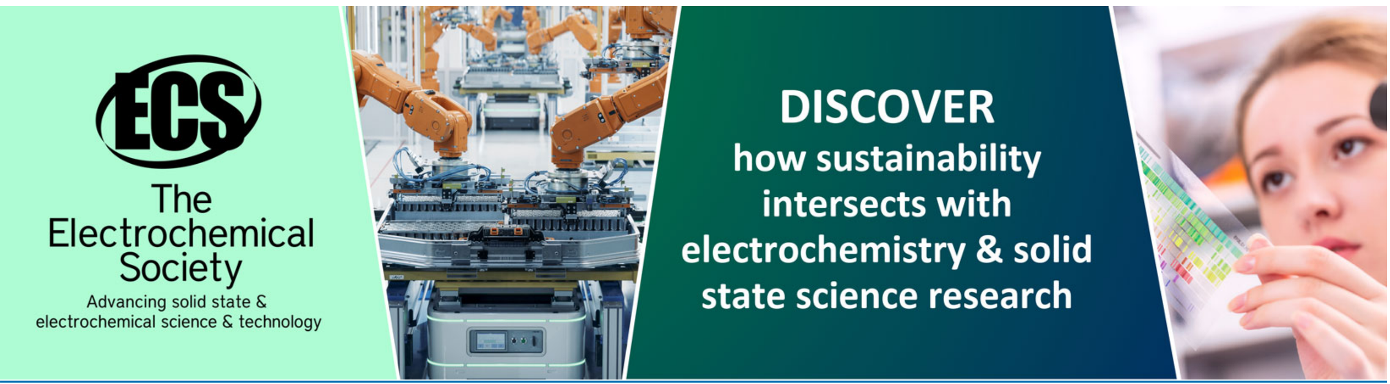

Numerical investigation of volume of fluid and level set interface capturing methods for bubble growth and detachment

Abdulaleem Albadawi[1], Yan Delauré[1], David B. Donoghue[2], Anthony Robinson[2] and Darina B. Murray[2]

[1] School of Mechanical and Manufacturing Engineering, Dublin City University, Ireland
[2] Department of Mechanical and Manufacturing Engineering, Trinity College Dublin, Ireland

E-mail: abdulaleem.albadawi2@mail.dcu.ie

E-mail: yan.delaure@dcu.ie

Abstract.

The injection of an air bubble in a liquid at rest is an interface flow problem where surface tension and its modeling at solid boundaries is a key factor. It is the subject of this study. Numerical simulations have been performed to study 3D axi-symmetrical bubble growth from an orifice through a horizontal wall. The gas inflow velocity used was sufficiently small to ensure that the bubble growth is quasi-static so that surface tension and buoyancy forces are dominant. The wall was considered non-wettable to avoid spreading of the interface along the wall. The Navier-Stokes equations were solved with two different interface capturing methods based on Volume of Fluid (VOF) and Level Set (LS) as well as coupled CVOFLS. In the VOF method, the bubble interface was tracked using either an algebraic solver which results in some diffusion of the interface (compressive scheme implemented in OpenFOAM), or it was determined using a geometric reconstruction scheme (Geo-Reconstruct Scheme from Fluent). The TransAT code was used for the LS model which captures the interface using signed distance function.

The bubble volume and center of gravity have been investigated during the growth using the three solvers and numerical results have been assessed against experimental data. These results have shown that reconstructing the interface using the LS method gives good agreement with the experiments. In VOF (compressive scheme), the bubble detaches at earlier times resulting in a smaller detachment volume. The coupled CVOFLS-GeoReconstruct was found to be more computationally expensive than the VOF-GeoReconstruct and to present bubble oscillation during the growth.

1. Introduction

Two phase flows are commonly found in a broad range of industrial applications such as heat exchangers, chemical processing, and electronic cooling. Bubbles are known, for example, to induce rapid and lasting increase in surface heat flux when sliding along heated plates [1]. The gas phase may originate from nucleation sites due to boiling or it can be directly injected into the system. The research presented in this article is concerned with the numerical study of the latter case of bubble injection for heat transfer enhancement applications as an initial stage of studying the full process of bubble growth, rise, and sliding. The analysis aims to examine the suitability of the models for predicting the bubble dynamics under adiabatic conditions. The main challenge of this analysis is that the bubble passes through different topological changes during its growth as the bubble is controlled by a balance between the buoyancy and capillary forces [2]. Fixed grid methods, in particular the VOF [3] and the LS [4] methods, make it possible to study the complex gas/liquid interface, by modeling both fluids as a single mixture. Recently, a coupling of the VOF and LS methods has also been developed (CVOFLS [5]) to achieve a smooth interface reconstruction while preserving mass conservation. Differences across the methods concern the interface advection but also its reconstruction which is used to evaluate fluid properties and critically the surface tension through the interface curvature.

Although most surface tension models are based on the same CSF method [ref], differences in their implementation, whether it is within the fluid domain or at boundaries where a triple contact point exists, can induce significant variations in the model predictions. The VOF method, for instance, is known to be affected by spurious currents induced by the curvature approximation [6]. The only existing study that has investigated the accuracy of both LS and VOF considered slug and bubbly flows [7] and no comparative study of the three methods (VOF, LS and CVOFLS) involving an assessment against experimental data has yet been published. The present research examines, using the three interface capturing methods, the capillary dominant flow of bubble growth at low Capillary and Bond numbers so that the implementation of the surface tension has a significant influence on the bubble dynamics and can lead to non negligible errors. The numerical prediction of bubble growth has been studied using either the VOF method [8, 9] or the LS method [10, 11], and recently the coupled CVOFLS method [12, 13, 14]. This body of research, however, has focused on the study of bubble perioding using high flow rates ($> 100mm^3/s$) [15, 14] and not low Capillary and Bond numbers. Also, previous studies have been concerned with predicting the bubble characteristics at detachment rather than the bubble shape and its characteristics during the growth which has a strong influence on determining the final bubble shape. Finally, the behavior of the bubble neck has been investigated previously using either experimental observations [16] or theoretical analysis of the inviscid pinch-off [17, 18] but is studied here by solving the full numerical domain where both gas and liquid viscosities.

The bubble formation is modeled using adiabatic axi-symmetrical conditions. The inflow flow rate is chosen so that isolated bubbles are generated from the wall orifice. The air is injected through an orifice wall where a static contact angle is imposed to pin the bubble interface at the orifice rim. This angle can have a strong influence on the bubble growth and detachment [11]. The accuracy of prediction of the neck formation, bubble detachment time and volume, the bubble aspect ratio, and the center of gravity in the gravitational direction are assessed by comparison against experimental data.

2. Governing equations and numerical analysis

Navier Stokes equations are solved to model the multiphase flows problem by treating the fluids as a single mixture.

$$\nabla \rho \vec{u} = 0 \tag{1}$$

$$\frac{\partial}{\partial t}(\rho \vec{u}) + \nabla \cdot (\rho \vec{u}\vec{u}) = -\nabla P + \nabla \cdot [\mu(\nabla \vec{u} + \nabla \vec{u}^T)] + \rho \vec{g} + \vec{F_\sigma} \tag{2}$$

where $\vec{u}$, p, ρ, μ, and $\vec{g}$ are mixture velocity, pressure, mixture fluid density, mixture fluid viscosity, and gravitational acceleration, respectively. The physical properties of both fluids are calculated each time step according to the interface position. The source term $\vec{F_\sigma}$ accounts for the surface tension. Its definition depends on the interface capturing method.

VOF method: In the VOF method, the volume fraction function is defined as a step function. It lies in the range $[0, 1]$. The liquid and the gas phases fill cells where $\alpha = 1$ and $\alpha = 0$, respectively. The cells, which contain a volume fraction between 0 and 1, include the interface. The volume fraction satisfies the advection equation $((\partial\alpha/\partial t) + \vec{u} \cdot \nabla\alpha = 0)$.

Two methods have been considered for the solution of the last equation; VOF-GeoReconstruct which uses the geometrical reconstruction method (PLIC-VOF [19]) implemented in Fluent, and VOF-compressive which is based on an analytical counter-gradient transport method [20]) implemented in OpenFOAM. In the GeoReconstruct model, the surface tension force model used is the Continuum Surface Force (CSF) model proposed by Brackbill et al. [21]:

$$F_\sigma = (\sigma\rho\kappa\nabla\alpha)/(1/2(\rho_g + \rho_l)) \tag{3}$$

where σ is the surface tension coefficient, κ is the interface curvature which is calculated in terms of the unit interface normal $\kappa = \nabla \cdot \hat{n} = \nabla \cdot (\nabla\alpha/|\nabla\alpha|)$. The subscripts g and l stand for the gas and the liquid, respectively. The surface tension force in OpenFOAM is calculated without using any density weighting ($F_\sigma = \sigma\kappa\nabla\alpha$).

LS method: In the LS method, the two immiscible fluids are characterized using a smoothed distance function ϕ , where the bubble free surface is defined by the isoline $\phi = 0$. After few time steps, the LS function fails to maintain the signed distance function $|\nabla\phi| \neq 1$. To solve this issue, a reinitialization (re-distancing) process is applied [4]. Furthermore, a Dirac function $\delta(\phi)$ is employed to limit the region where the surface tension force is considered.

$$f_\sigma = \sigma\kappa(\phi)\delta(\phi)\nabla\phi \tag{4}$$

CVOFLS-GeoReconstruct: In this case, both the LS and the VOF advection equations are solved. The re-initialization is accomplished by using the PLIC reconstruction. The interface normal is determined using the LS function, while the fluid volume is obtained from the VOF function. The surface tension force and the physical properties are calculated similarly to the LS method.

Numerical solution: A cell center finite volume formulation is used to discretize the governing equations. The temporal derivative parameters are discretized using a first order Euler implicit scheme, while the spatial derivatives are discretized using second order schemes.TransAT uses SIMPLE algorithm [22] for coupling between the velocity and the pressure. This coupling is attained in both Fluent and OpenFOAM by using PISO algorithm [23].

3. Problem description

The bubble is injected through an orifice with a radius $r_o = 0.8 \times 10^{-3}m$ submerged into an initially quiescent liquid (Figure 1). The gravitational acceleration is imposed in the axi-symmetrical direction, while the surface tension coefficient is assumed to be constant ($0.073kg/s^2$). The physical properties of both air ($\rho = 1.225kg/m^3, \mu = 1.789 \times 10^{-5}kg/(m.s)$) and water ($\rho = 998.2kg/m^3, \mu = 1.003 \times 10^{-3}kg/(m.s)$) are constant and taken at room temperature. The gas is injected under constant flow rate ($\dot{Q} = 100mlph = 27.778 \times 10^{-9}m^3/s$) which is well below the critical value for quasi-static flow [24] ($\dot{Q}_{crit} \approx \pi(\frac{16}{3g^2})^{1/6}(\frac{\sigma_L r_o}{\rho_L})^{5/6} = 1.82 \times 10^{-6}m^3/s$). The numerical domain has a width $\sim 2.5D_{eq}$ and height $\sim 5D_{eq}$, equivalent to $10 \times 20mm^2$. The wall dimensions chosen in this study are comparable with Gerlach et al. [12]. The mesh step size is regular $\Delta x = 0.1 \times 10^{-3}m$, so that the orifice diameter will be simulated using 16 grid cells. The time step was chosen small enough, $\Delta t = 1 \times 10^{-5}s$ to give Courant number below 0.4. The step sizes are relatively close to those taken in other studies [12, 25]. Four boundary conditions are set to represent the borders of the numerical domain. Inflow velocity is defined at the inlet where the gas is injected through the throat at a constant velocity. The velocity is determined according to the imposed volumetric flow rate $v_0 = \dot{Q}/(\pi r_0^2) = 0.0138m/s$. A no slip wall boundary condition is imposed along all walls except for the lower wall where wall adhesion is considered. A contact angle is defined so that the bubble interface will not spread along the wall. The numerical results are compared with the experimental data produced using the experimental setup described in [26].

4. Results and Discussion

4.1. Dynamics of Bubble Formation

Figure 2 shows the bubble interface at 5 successive stages of growth ($t/t_{det} \sim 0, 0.2, 0.4, 0.6, 0.8, 1$, where t_{det} is the detachment time) as modelled by the LS method and measured experimentally. The other methods provide bubble shapes which are broadly similar. With LS and CVOFLS, the interface is captured by the isoline $\phi = 0$, while the interface is represented in VOF by the isoline $\alpha = 0.5$. At the initial stage $t/t_{det} \sim 0$, the bubble is assumed to have a hemispherical shape with a stationary gas. At time $t/t_{det} \sim 0.2, 0.4$, the bubble has a truncated spherical shape where the bubble growth is dominated by the capillary force $\sim 2\pi\sigma r_o$ [2]. As the bubble grows, the buoyancy force ($\sim (\rho_l - \rho_g) g V_B$) increases and has a larger influence on the formation. From that stage, the bubble becomes spherical, and the balance between capillary and buoyancy forces controls the bubble growth. At larger times $t/t_{det} \sim 0.8$, the bubble becomes more elongated leading to increased instantaneous contact angle and a neck formation. At time $t/t_{det} = 1$, the bubble detaches where the neck pinches off, and it rises freely due to the gravitational effect.

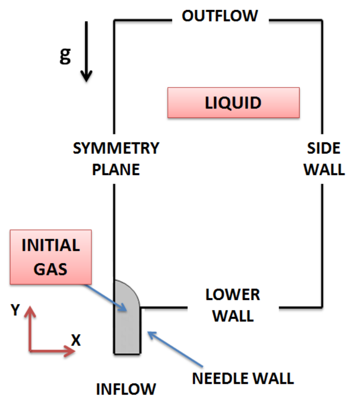

Figure 1. Schematic diagram of the numerical rig.

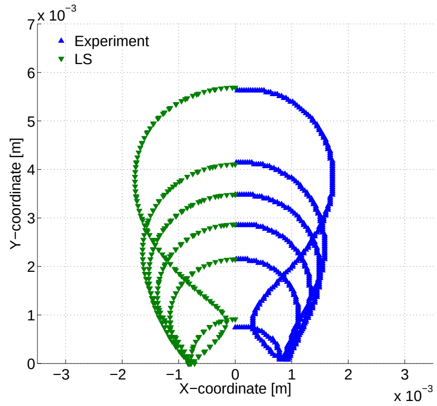

Figure 2. History of the bubble shape using LS method and experimental data.

4.2. Bubble detachment parameters

The numerical methods are first assessed by comparing the geometrical parameters at detachment with experimental data. Results are summarized in table 1 and indicate that the LS and the VOF-GeoReconstruct methods tend to give the largest detachment volume with an error $\frac{V_{num}-V_{exp}}{V_{exp}} \times 100 < 7\%$. Although this is non negligible, the error from the equivalent bubble radius defined as $R = (3V_{det}/4\pi)^{1/3}$ is small $\sim 2.1\%$. VOF-Compressive gives very small detachment volume by comparison with the experiments with an early bubble detachment (see Table 1 for the detachment time). The VOF-GeoReconstruct and LS solvers, on the other hand, provide larger detachment time when compared to the experimental data. All the numerical methods except VOF-Compressive give detachment center of gravity close to the experimental measurements with difference smaller than $1.5\Delta x$. The detachment parameters show that the only method which does not predict accurately the bubble characteristics at detachment is the algebraic advection scheme (VOF-Compressive).

4.3. Bubble Geometrical Aspects

The history of bubble growth is studied in this section to investigate the unsteady growth and detachment process. Figure 3 shows the numerical and the experimental results of the bubble

Method	Volume $[mm^3]$	Error(%)	Center of Gravity $[mm]$	Error(%)	Time $[s]$	Error(%)
Experiment	26.98		3.513		0.954	
VOF-GeoReconstruct	28.863	06.979	3.385	-03.635	0.997	04.476
CVOFLS-GeoReconstruct	27.215	00.871	3.423	-02.559	0.937	-01.824
LS	28.786	06.694	3.566	01.503	1.005	05.293
VOF-Compressive	20.234	-25.004	3.068	-12.673	0.606	-36.478

Table 1. Numerical and experimental bubble detachment parameters and the corresponding error.

center of gravity in the vertical direction CGy. The VOF-Compressive method shows a rapid increase in stretching along the vertical direction before detachment. This occurs at time $t = 0.4s$ instead of $t = 0.9s$ with other methods. The LS method shows a bubble which grows smoothly until detachment as observed experimentally. Also, although the CVOFLS-GeoReconstruct method gives detachment center of gravity which agrees with experimental measurments, it predicts bubble oscillations during the growth with amplitude of oscillation which increases towards detachment. The bubble aspect ratio provides further details on the dynamic behavior of the bubble shape. It is defined as the ratio of the maximum bubble height to the maximum bubble width and is shown in figure 4. In VOF-Compressive, the bubble grows faster in the longitudinal direction than the horizontal. The instability of the Geo-Reconstruct methods is further exhibited in this figure. This behavior is represented by a Pulse-Shrink motion, where the growth is accompanied by a rhythmical expansion and contraction of the bubble. Similar observations are noticed when examining the instantaneous contact angle behavior during the growth (Figure 5). This contact angle is defined as the angle between the tangential wall axis and the gas/liquid interface, and is measured in the heavier phase (water). At the onset of bubble growth, it decreases until reaching a minimum value where the bubble has a truncated spherical shape. The angle is then shown to increase as the bubble elongates in the vertical direction. The neck formation and detachment stage is determined by the rapid increase of the contact angle. Duhar and Colin [2] observed similar behavior of this angle in their experimental data.

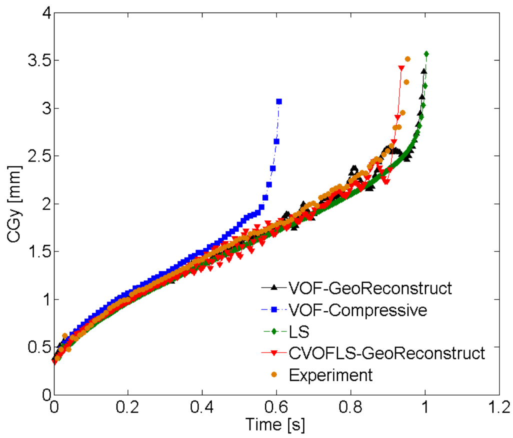

Figure 3. Comparison between the numerical and the experimental results for the bubble center of gravity.

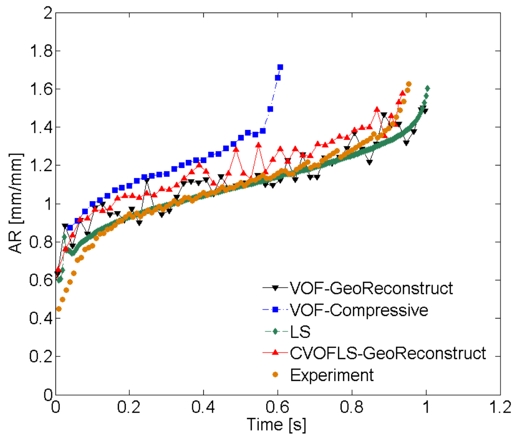

Figure 4. Comparison between the numerical and the experimental results for the aspect ratio.

Figure 6 displays the neck radius during detachment. The origin of the horizontal axis is defined at the moment when the bubble breaks-up. In spite of the apparent difference in the geometrical properties during the bubble growth between the different methods, the bubble follows the same behavior during the neck break-up. The neck radius starts to decrease rapidly at time $0.01s$ before detachment. The onset of the neck formation is assumed to be when the minimum bubble radius is smaller than the orifice radius, while the bubble detaches when the neck radius reaches the mesh step size. The logarithmic scale plot of the neck radius is shown to follow an exponential law $R_{neck} \propto c(-t_{det})^{\gamma}$ at the final stages of the bubble break-up where the logarithmic curve is linear. This behavior was previously observed [18, 16]. The exponential power has an approximate value of 0.3. Based on Rayleigh-Plesset equation, Gordillo [18] showed that the minimum bubble radius follows either a logarithmic law $t_{det} \propto R_{neck}^2\sqrt{-lnR_{neck}^2}$)where the neck has a slender shape before detachment, or an exponential law $R_{neck} \propto c(-t_{det})^{\gamma}$with $\gamma = 1/3$ where the neck divides the bubble into two cones with different semi-angles. The formation of the neck forces the gas inflow to pass through narrower region. This increases the velocity of the gas stream through the neck leading to a pressure suction inside the neck (Bernoulli effect). The large pressure difference generated at the neck between the inner gas and the outer liquid draws the liquid towards the neck and accelerates the bubble break-up.

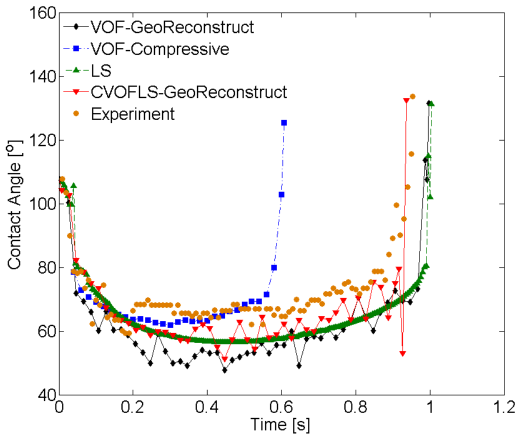

Figure 5. Comparison between the numerical and the experimental results for the bubble instantaneous contact angle.

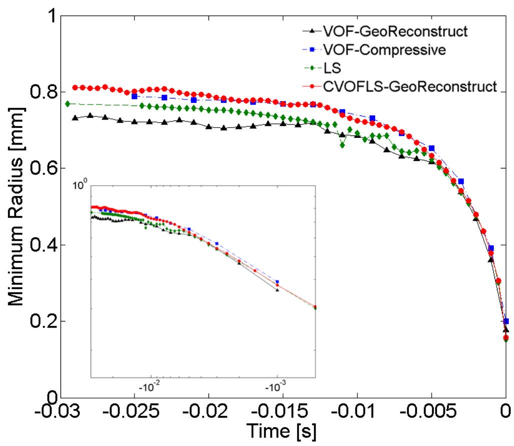

Figure 6. Comparison of the minimum bubble radius (Neck radius) during the detachment.

4.4. Surface tension modeling

The main difference between the numerical methods relates to the modeling of surface tension. In VOF-Compressive, it is based on the CSF model which generates large velocities inside the bubble. It is possible that these velocities are the reason of the non-physical detachment. Although Fluent also uses CSF model in VOF-GeoReconstruct, the surface tension force model is dampened using an averaged density (see Eqn. 3). The density averaging is localising the surface tension towards the liquid phase where its influence is significantly smaller due to the large density of the liquid. A different scheme is implemented by the LS and CVOFLS methods. The surface tension term (eqn. 4) in this case is applied only over a narrow region around the interface by using the Dirac (delta) function. Furthermore, the physical properties are smoothly distributed across the interface in the CVOFLS and the LS methods since the mixture density is

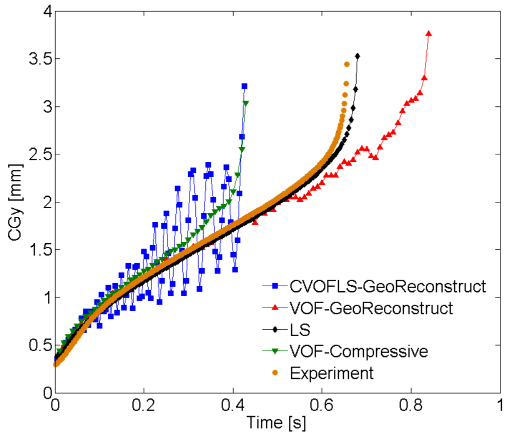

Figure 7. Center of Gravity profile for inflow flow rate $150mlph$ and orifice diameter $1.6mm$.

calculated using a smoothed Heaviside function rather than a step function (volume fraction α). The static contact angle formulation has been used with all the methods as a boundary condition for both the VOF and LS fields. The imposed static contact angle corrects the interface normal at the cells close to the wall and as a result the bubble interface curvature at the adjacent cells to the wall. This correction can impose large and sudden variations in the instantaneous contact angle between the first and the second cells in the direction perpendicular to the wall. This can enhance the large oscillations that are observed, in particular with the GeoReconstruct methods. Such oscillations can lead to an earlier detachment and to a non-stable bubble rise by changing the conditions at detachment.

4.5. Influence of flow rate
The LS method studied in this research has been shown to give physically consistent results. Higher volumetric flow rate was considered here ($150mlph$) to confirm the last results. In this case, the detachment parameters (except the time) should remain the same since it is a quasi-static flow. The larger volumetric flow rate, however, induces significant gas circulations inside the bubble with a corresponding increase in Courant number ($U\Delta t/\Delta x$). Hence, any unphysical results will be more apparent. Figure 7 shows the profile of bubble CGy during the growth for the volumetric flow rate $150mlph$. For the GeoReconstruct methods, the discrepancy between the experimental and the numerical data increases with increasing flow rate. CVOFLS-GeoReconstruct gives unphysical oscillations larger than what is observed with $100mlph$. Althought VOF-GeoReconstruct gives stable results, it detaches with larger center of gravity. The best results were obtained again using the LS method where the center of gravity is always the closest to the experimental data. The results also highlighted that increasing the flow rates leads to higher sensitivity to the time step and the solution residuals.

5. Conclusions
The quasi-static bubble growth and detachment through an orifice submerged into a quiescent liquid were investigated using four different interface capturing methods (VOF-Compressive, VOF-GeoReconstruct, CVOFLS-GeoReconstruct, and LS). For $100mlph$, all the numerical methods except the VOF-Compressive were in good agreement with the experimental results for the detachment volume, time, and center of gravity. Results suggested that the difference in the implementation of the surface tension force in each method was the main contributing

factor in the difference at detachment. The GeoReconstruct methods were showen to give bubble oscillations during the growth, this oscillation is deemed to be due to the implementation of the static contact angle model. During detachment, the neck radius decreases rapidly and follows an exponential power law at the final stages of detachment. The exponential power was found to be (0.3) which is smaller than the value predicted by Rayleigh-Plesset equation (1/3). The Bernoulli effect was explained to be the result of the rapid neck break-up. For the prescribed conditions and by using higher inflow flow rates, the LS method proved to provide the most precise and stable detachment results.

Acknowledgments
The authors wish to acknowledge the support of Science Foundation Ireland under its Research Frontiers Programme (grant number 09/RFP/ENM2151).

References

[1] Delauré Y M C, Chan V S S and Murray D B 2003 *Exp. Therm. Fluid Sci.* **27** 911–926
[2] Duhar G and Colin C 2006 *Phys. Fluids* **18** 077101
[3] Hirt C W and Nichols B D 1981 *J. Comput. Phys.* **39** 201–25
[4] Sussman M, Smereka P and Osher S 1994 *Journal of computational Physics* **114** 146–59
[5] Sussman M and Puckett E G 2000 *J. Comput. Phys.* **162** 301–37
[6] Renardy Y and Renardy M 2002 *J. Comput. Phys.* **183** 400–421
[7] Carlson A, Kudinov P and Narayanan C 2008 *5th European Thermal-Sciences Conf., The Netherlands*
[8] Li Y, Yang G, Zhang J and Fan L S 2001 *Powder Technol.* **116** 246–260
[9] Ma D, Liu M, Zu Y and Tang C 2012 *Chemical Engineering Science* **72** 61–77
[10] Chen C and Fan L S 2004 *AIChE Journal* **50** 288–301
[11] Chen Y, Mertz R and Kulenovic R 2009 *Int. J. Multiphas. Flow* **35** 66–77
[12] Gerlach D, Alleborn N, Buwa V and Durst F 2007 *Chem. Eng. Sci.* **62** 2109–25
[13] Buwa V V, Gerlach D, Durst F and Schlcker E 2007 *Chem. Eng. Sci.* **62** 7119–7132
[14] Chakraborty I, Biswas G and Ghoshdastidar P 2011 *Int.l J. Heat Mass Tran.* **54** 4673–88
[15] Ohta M, Kikuchi D, Yoshida Y and Sussman M 2011 *Int. J. Multiphas. Flow* **37** 1059–71
[16] Thoroddsen S, Etoh T and Takehara K 2007 *Physics of Fluids* **19** 042101
[17] Bolanoz-Jimenéz R, Sevilla A, Martnez-Bazn C and Gordillo J 2008 *Phys. Fluids* **20** 112104
[18] Gordillo J, Sevilla A, Rodrguez-Rodrguez J and Martnez-Bazn C 2005 *Phys. Rev. Lett.* **95** 194501
[19] Youngs D L 1982 *Numerical methods for fluid dynamics* **1** 41–51
[20] Weller H G 2008 A new approach to vof-based interface capturing methods for incompressible and compressible flows, Tech. rep. no. TR/HGW/04
[21] Brackbill J, Kothe D and Zemach C 1992 *J. Comput. Phys.* **100** 335–54
[22] Patankar S V and Spalding D B 1972 *Int. J. Heat Mass Tran.* **15** 1787–06
[23] Issa R 1986 *Journal of Computational physics* **62** 40–65
[24] Oguz H N and Prosperetti A 1993 *Journal of Fluid Mechanics* **257** 111–45
[25] Chakraborty I, Ray B, Biswas G, Durst F, Sharma A and Ghoshdastidar P 2009 *Physics of Fluids* **21** 062103
[26] Donoghue D B, Delauré Y M C, Robinson A J and Murray D B 2011 *Proc. of the 6th Baltic Heat Transfer Conf., Tampere, Finland*